



RESEARCH ARTICLE

A tumor-targeting cRGD-EGFR siRNA conjugate and its anti-tumor effect on glioblastoma *in vitro* and *in vivo*

Shuai He^{1,2*}, Bohong Cen^{1*}, Lumin Liao¹, Zhen Wang¹, Yixin Qin¹, Zhuomin Wu¹, Wenjie Liao¹, Zhongyi Zhang¹, and Aimin Ji^{1,2}

¹Department of Pharmacy, Zhujiang Hospital of Southern Medical University, Guangzhou, China and ²Guangdong Provincial Key Laboratory of New Drug Screening, School of Pharmaceutical Sciences, Southern Medical University, Guangzhou, China

Abstract

The epidermal growth factor receptor (EGFR) is an important anti-tumor target. The development of novel molecular-targeted anti-tumor drugs that can target the interior of tumor cells and specifically silence EGFR expression is valuable and promising. In this work, a promising anti-tumor conjugate comprising methoxy-modified EGFR siRNA and cyclic arginine-glycine-aspartic acid (cRGD) peptides, which selectively bind to $\alpha v\beta 3$ integrins, was synthesized and examined. To prepare cRGD-EGFR siRNA (cRGD-siEGFR), cRGD was covalently conjugated to the 5'-end of an siRNA sense strand using a thiol-maleimide linker. The cellular uptake and cytotoxicity of cRGD-siEGFR *in vitro* were tested using an $\alpha v\beta 3$ -positive U87MG cell line. *In vivo* bio-distribution, anti-tumor activity, immunogenicity and toxicity were investigated in a nude mouse tumor model through repeated i.v. administration of cRGD-siEGFR (7 times over a 48 h interval). Analyses of *in vitro* data showed that cRGD-siEGFR silenced EGFR expression effectively, with high tumor targeting ability. Administration of cRGD-siEGFR to tumor-bearing nude mice led to significant inhibition of tumor growth, obvious reduction of EGFR expression and down-regulation of EGFR mRNA and protein in tumor tissue. Furthermore, serum biochemistry and pathological section evaluation did not indicate any serious toxicity of cRGD-siEGFR *in vivo*. cRGD-siEGFR is likely a promising candidate with high targeting ability, substantial anti-tumor effects and low toxicity *in vitro* and *in vivo*.

Keywords

siRNA delivery, conjugate system, tumor targeting, gene silencing, glioblastoma

History

Received 22 September 2016

Revised 21 November 2016

Accepted 29 November 2016

Introduction

Glioblastoma (GBM; WHO grade IV astrocytoma) is the most common and aggressive primary malignant tumor of the CNS (Louis, 2006). Current conventional treatments for glioblastoma include surgery, radiotherapy and chemotherapy, while treatment effects are limited, with adverse reactions and injury to the human body. Recently, novel molecular-targeting drugs have been applied as a primary approach to glioblastoma treatment and exhibit high specificity, lower toxicity and fewer side effects and good tolerance (Le Tourneau et al., 2015; Cetin et al., 2016).

Epidermal growth factor receptor (EGFR) has been shown to be overexpressed in a variety of tumors and is one of the

significant factors responsible for the development of gliomas. The EGFR tyrosine kinase inhibitors (EGFR-TKIs) have become an important focus for tumor-related drug development (Xu et al., 2016), such as small-molecule targeted drugs (Maemondo et al., 2010; Horiike et al., 2014; Liang et al., 2014; Choi et al., 2015), monoclonal antibodies (Hudis, 2007; Jonker et al., 2014; Pietrantonio et al. 2013) and cancer vaccines (Guo et al., 2013; Ahmed & Bae, 2014). However, small-molecule targeted inhibitors and monoclonal antibody drugs cause several adverse reactions, primarily because EGFR expression is suppressed in normal cells in addition to tumor cells. Drug resistance is primarily related to EGFR-associated proteins that are prone to isomerization, thereby reducing the binding of the drug. Therefore, the development of novel tumor-targeting drugs for EGFR has become more and more urgent.

Previous studies have shown that the $\alpha v\beta 3$ integrin receptor is highly expressed on the cell surface in multiple malignant tumors and tumor blood vessels, while barely expressed in normal cells and tissues (Shimaoka et al., 2003; Wang et al., 2016). Small interfering RNA (siRNA) has great therapeutic potential for cancers caused by abnormal gene overexpression or mutations *via* sequence-specific post-transcriptional gene silencing (Shen et al., 2014). However,

*The first two authors should be regarded as joint first authors.

Address for correspondence: Aimin Ji, Department of Pharmacy, Zhujiang Hospital of Southern Medical University, Guangzhou 510282, China. Tel: +86 20 61643500. Email: aiminji_007@163.com
Zhongyi Zhang, Department of Pharmacy, Zhujiang Hospital of Southern Medical University, Guangzhou 510282, China. Tel: +86 20 62783372. Email: zjyycp@163.com

This is an Open Access article distributed under the terms of the Creative Commons Attribution License (<http://creativecommons.org/licenses/by/4.0/>), which permits unrestricted use, distribution, and reproduction in any medium, provided the original work is properly cited.

to activate the RNAi pathway, siRNA molecules require safe and efficient delivery systems, such as nanoparticles and conjugates (Shen et al., 2013; Liu et al., 2014), which enable prolonged circulation *in vivo*, high accessibility to target cells and optimized cytosolic release after efficient cellular uptake (Li et al., 2016). In our previous studies (Liu et al., 2014), cRGD-Vegfr2 siRNA conjugates were synthesized. *In vitro* and *in vivo* studies showed that cRGD-Vegfr2 siRNA could silence the expression of Vegfr2 mRNA and inhibit tumor angiogenesis.

However, little effort has been spent on the development of suppressing EGFR expression with siRNA conjugates for glioblastoma therapy. Here, cRGD-siEGFR conjugates have been synthesized, based on the high affinity of integrin $\alpha\beta3$ to cRGD (Dechantsreiter et al., 1999). A cRGD peptide was covalently attached to the end of a sense strand of siRNA, which silences EGFR mRNA. The anti-tumor effect of cRGD-siEGFR was observed *in vitro* and *in vivo*, including the specific silencing effect, tumor targeting ability, anti-tumor growth activity, toxicity and immune stimulation reaction. Moreover, the feasibility and shortcomings of cRGD-siEGFR for use as a novel molecular-targeted anti-tumor drug were systematically investigated.

Compared with the current small-molecule targeted inhibitors and monoclonal antibody drugs, cRGD-siEGFR may have some beneficial characteristics, such as better tumor targeting and fewer side effects. In addition, cRGD-siEGFR could elicit less drug resistance by inhibiting EGFR expression at the gene level. It could be a valuable and promising way to develop novel molecular-targeted anti-tumor drugs that specifically silence EGFR expression (Lee et al., 2015).

Materials and methods

Materials

U87MG (human malignant glioblastoma multiforme cell line, ATCC® number: HTB-14). HeLa cells were kindly provided by Department of Hematology, Zhujiang Hospital, Southern Medical University (Guangzhou, China). Cells were grown and cultured using supplier recommended reagents and media according to the standard protocols and procedures.

SYBR® Premix Ex Taq™ and PrimeScript™ RT reagent Kit with gDNA Eraser (TaKaRa, Kusatsu city, Japanese), 100 bp DNA Ladder (Genscript, Piscataway, NJ, Cat.No.M102R), Trizol reagent and Lipofectamine 2000 (Invitrogen, Carlsbad, CA). Novex® ECL Chemiluminescent Substrate Reagent (Invitrogen). Monoclonal anti-mouse EGFR/Fik-1 antibody (R&D, Shanghai, China), Primary monoclonal anti-integrin $\alpha\beta3$ antibody (eBioscience, San Diego, CA, Catalog Number: 11-0519), D-Luciferin (BioVision, Milpitas, CA)/ELISA kit (eBioscience).

siRNA sequence backbone modifications and verification

siRNA sequences for experiments:

Human EGFR siRNA (Sense strand: 5'-CAAAGUGUGU AACGGAAUAdTdT-3'; Anti-sense strand: 5'-UAUCCGU UACACACUUUGdTdT-3')

Negative control siRNA (Sense strand: 5'-AUCGAAUUC CUGCAGCCCGUUdTdT-3'; Anti-sense strand: 5'-AACGG GCUGCAGGAAUUCGAUdTdT-3')

Mouse Vegfr2 siRNA (Sense strand: 5'-CGGAGAAGAA UGUGGUUAAAdTdT-3'; Anti-sense strand: 5'-UUAACCAC AUUCUUCUCCGdTdT-3')

Primer sequences for qRT-PCR analysis:

Human EGFR (Forward primer: 5'-GCCGCAAAGTGTG TAACGGAAATAG-3'; Reverse primer: 5'-TGGATCCAGAG GAGGAGTATGTGT-3')

Human GAPDH(Forward primer: 5'-CGGAGTCAACGG ATTTGGTCTGAT-3'; Reverse primer: 5'-AGCCTTCTCCA TGGTGGTGAAGAC-3')

Indodicarbocyanine-5 (Cy5)-labeled siRNA (siRNA-Cy5) and all of the abovementioned siRNAs were purchased from Guangzhou RiboBio Co., Ltd.

The relative expression level of EGFR mRNA was tested by qRT-PCR. In order to improve the stability, reduce the immunogenicity and off-target effect, EGFR siRNA sequence was modified as seen in Table S1.

Synthesis of cRGD-siEGFR

To prepare cRGD-siRNA molecules, cyclic RGD was covalently conjugated to the 5'-end of an siRNA sense strand using a thiol-maleimide linker. The synthetic process was performed as previously described (Liu et al., 2014). The molecular weight of cRGD-sense strand siRNA was characterized by Oligo HTCS LC-MS system (Novatia, Newtown, Pennsylvania). The purity of conjugated cRGD-siRNA was determined by HPLC. The analyses were performed employing an Agela C-8 column (25 cm × 4.6 mm) according to the following conditions: starting from 0.1 M triethylammonium acetate pH 7.4, a linear gradient of 0%–50% MeCN was pumped at a flow rate of 1 mL/min for 0 min–30 min.

Serum stability of cRGD-siEGFR and EGFR siRNA

To improve the stability, the EGFR siRNA sequence was modified, as seen in Table S1. Five microliters of 20 μ M cRGD-siEGFR or EGFR siRNA was mixed with 5 μ L of mouse serum and incubated at 37 °C for 0, 12, 24, 36 and 48 h. Aliquots were taken at each of the time points and subjected to electrophoresis in 1.2% non-denaturing agarose gels.

qRT-PCR and western blot analysis

The qRT-PCR and western blot analysis were conducted as previously described (Liu et al., 2014).

Cytotoxicity analysis *in vitro*

Cells were seeded into 96-well microtiter plates (BD Falcon) at a density of 4×10^4 cells/well and allowed to attach for 24 h. cRGD-Nonsense Control siRNA (cRGD-siNC) at concentrations of 100, 200, 500, 1000, 1500 and 2000 nM (final concentration) were added into different wells in triplicate and incubated with cells for 24 h, 48 h and 72 h, according to the manufacturer's protocols. Then, 10 μ L of Cell Counting Kit-8 (Dojindo, Japan) solution was added to each well. Plates

were incubated at 37 °C for an additional 1 h, and optical densities were recorded at 450 nm using a microplate reader (Bio-Rad, Hercules, CA). Cell viability was plotted as a percentage of untreated control cells.

The expression level of integrin $\alpha v \beta 3$

U87MG cells were transfected with Cy5-labeled cRGD-siEGFR, Cy5-labeled siRNA and Lipo2000/siRNA-Cy5 complexes in Dulbecco's modified Eagle's medium (DMEM) containing 10% fetal bovine serum (FBS). To demonstrate the effect of cRGD binding to the $\alpha v \beta 3$ receptor, the U87MG cells were also pre-treated with 1 μ M of un-conjugated cRGD peptide (cRGD blocked) for 30 min at 37 °C prior to transfection with cRGD-siEGFR-Cy5, as shown in a previous report (Alam et al., 2011). The final concentration of the compound was 100 nM. Six hours after transfection, cells were washed with PBS and fixed immediately using 4% paraformaldehyde at room temperature for 15 min, followed by nuclear staining with 4,6-diamidino-2-phenylindole (DAPI) (Roche, Switzerland) for 10 min at 37 °C. Cells were imaged with confocal microscopy (Olympus, Tokyo, Japan; Cy5 excitation = 640 nm, emission = 680 nm).

Cellular uptake level

U87MG cells were incubated with different concentrations of cRGD-siEGFR-Cy5 (100 nM or 400 nM) and Lipo2000/siRNA-Cy5 complexes (100 nM) for 6 h at 37 °C. Then, the cells were washed with PBS three times to remove any extracellular cRGD-siEGFR-Cy5 or siRNA-Cy5. Cells were collected and analyzed with a BD FACS Calibur Cell Sorting System (BD Biosciences, San Jose, CA). Data were obtained and analyzed using Cell Quest software.

Apoptosis analysis

Briefly, 72 h after siRNA transfection, U87MG cells were stained in accordance with the manufacturer's instructions. Adherent and floating cells were collected, stained with FITC-labeled Annexin V (eBioscience) and propidium iodide (eBioscience), and analyzed on a BD FACS Calibur Cell Sorting System (BD Biosciences).

Cell proliferation analysis by CCK-8 and 5-ethynyl-2'-deoxyuridine (EdU) assays

Cells were seeded into 96-well microtiter plates (BD Falcon, San Jose, CA) at a density of 4×10^4 cells/well and allowed to attach for 24 h. cRGD-siEGFR at concentrations of 0, 400, 600 or 800 nM (final concentration) were added into different wells in triplicate and incubated with cells for 48 h and 72 h, according to the manufacturer's protocols. Then, 10 μ L of CCK-8 (Dojindo, Japan) solution was added to each well. Plates were incubated at 37 °C for an additional 1 h and optical densities were recorded at 450 nm using a microplate reader (Bio-Rad). Cell viability was plotted as a percentage of untreated control cells. cRGD-siEGFR, at a concentration of 800 nM, was added and incubated with cells for 48 h. Then, 50 μ M EdU (Guangzhou Ruibo, China) solution was added to each well and incubated at

37 °C for an additional 2 h. EdU labeling and EdU staining were performed using a standard protocol (Salic & Mitchison, 2008). EdU-stained cells were counterstained with Hoechst and imaged with confocal laser scanning microscopy.

Tumor model establishment

BALB/c nude mice (female, 4–6 weeks old, ~20 g) were purchased from the Experimental Animal Center of Sun Yat-Sen University and maintained in a sterile environment, according to the standardized animal care guidelines. The experiments were performed according to the national regulations. Nude mice were inoculated subcutaneously on the right back with 5×10^6 U87MG cells. When tumor volume reached 150 mm³, the animals were randomized into different groups for anti-tumor activity. For bio-distribution and tumor vascular permeability experiments with cRGD-siRNA, 5×10^6 U87MG or HeLa cells were injected subcutaneously on the right back of nude mice, and experiments were performed when tumor volume reached 120 mm³.

In vivo distribution

Mice bearing U87MG tumors were injected intravenously with 1 nmol/20 g cRGD-siRNA-Cy5 or siRNA-Cy5 at single doses ($n = 4$). The subsequent bio-distribution was detected at 12 h, 24 h, 48 h and 72 h using an IVIS Spectrum imaging system at the appropriate wavelength (Cy5: $\lambda_{ex} = 640$ nm, $\lambda_{em} = 680$ nm). The tumors and major organs were excised and imaged at 24 h or 72 h.

Tumor vascular permeability

Mice bearing U87MG tumors were injected intravenously with cRGD-siRNA-Cy5 or siRNA-Cy5. Mice bearing HeLa tumors were injected with cRGD-siRNA-Cy5. Animals were euthanized 24 h after treatment. Immunofluorescence analysis was performed as previously described (Liu et al., 2014).

Anti-tumor activity

Mice bearing U87MG tumors were injected intravenously with cRGD-siEGFR 7 times over a 48 h interval with one of the following treatments. A: saline, B: cRGD-siNC (5 nmol/20 g), C: cRGD-Vegfr2 siRNA (1.5 nmol/20 g), D: cRGD-siEGFR (1.5 nmol/20 g), E: cRGD-Vegfr2 siRNA (1.5 nmol/20 g) + cRGD-siEGFR (1.5 nmol/20 g), F: cRGD-siEGFR (5 nmol/20 g). Tumor volumes were measured with a caliper before injection and calculated using the following formula: volume = $\frac{1}{2} \times \text{length} \times (\text{width})^2$, where length represented the longest tumor diameter and width represented the shortest tumor diameter. The growth curves were plotted as the mean tumor volume \pm SD (standard deviation). Animals were euthanized 3 days after the last treatment and the tumors and visceral organs were excised and preserved in liquid nitrogen for further analysis.

EGFR expression level was determined by qRT-PCR, western blot and immunohistochemistry. Tissue sections were processed for TUNEL analysis using an *in situ* cell death detection kit-POD (Roche) as a measure of apoptosis.

Toxicity and immunogenicity evaluation *in vivo*

For immune response studies, the serum was collected from C57BL/6J mice 6 h after injection of cRGD-siEGFR (5 nmol/20 g) or saline. IL-6, IL-12, IFN- α and IFN- γ levels in the serum were detected by ELISA. For toxicity studies, the serum was collected from mice bearing U87MG tumors that were injected intravenously with cRGD-siEGFR 7 times, and ALT (alanine aminotransferase) and Cr (creatinine) were measured with an automated Aeroset Chemistry Analyzer (Abbott, Abbott Park, IL), based on manufacturer's instructions.

Visceral organ toxicity check

For the visceral organ toxicity analysis, 3 days after the last of seven injections, the heart, liver, spleen and kidneys were excised from nude mice treated with cRGD-siEGFR (1.5 nmol/20 g), cRGD-siEGFR (5 nmol/20 g) or saline. Tumor tissues were fixed immediately using 4% paraformaldehyde. All the sections were stained with hematoxylin eosin (HE).

Statistical analysis

Statistical analysis of the data was performed through one-way analysis of variance (ANOVA) (SPSS software, version 19.0). The results are expressed as the mean \pm standard error, and $p < 0.05$ was considered statistically significant. All statistical tests were two-sided.

Results

Synthesis and serum stability of cRGD-siEGFR

A diagram of cRGD-siRNA conjugates is shown in Figure 1(A). The cRGD moiety was conjugated to the 5'-phosphate of a passenger strand of siRNA through a thiol-maleimide linker. HPLC-MS results showed that the molecular mass of synthesized cRGD-siEGFR was consistent with the theoretical molecular mass. The cRGD-conjugated sense strand siRNA was determined to be 7923.4 Da, which was acceptably close to the predicted mass of 7921.4 Da, as seen in Supplementary Figure S1(A). The RP-HPLC results showed that the purity of cRGD-siEGFR reached 88.0%, as seen in Supplementary Figure S1(B). For EGFR siRNA sequence and backbone modification verification, the silencing efficiency of EGFR siRNA-C was measured and determined to be over 80%, and the stability was obviously improved, without decreasing the silencing efficiency, by the use of three 2'-O-Me modifications on the both ends of the sense strand and antisense strand of siRNAs, as seen in Figure S1(C,D) and Table S1. Incubation of 2'-O-Me-modified cRGD-siRNA conjugates in mouse serum revealed very little degradation after 48 h. In similar conditions, unmodified RNA oligonucleotides were mostly degraded after 24 h, as seen in Figure S1(C).

Intracellular distribution of cRGD-siEGFR

To detect the intracellular distribution, cRGD-siEGFR conjugates were labeled with a fluorophore (Cy5). cRGD-siEGFR delivered siRNA into U87MG cells, while naked siRNA did not. When integrin $\alpha\beta 3$ receptor on the cell

surface was blocked by pre-incubation with cRGD, cRGD-siEGFR failed to enter cells, which suggested that cRGD-siEGFR was specifically taken up by glioblastoma cells *via* $\alpha\beta 3$ receptors (Figure 1B). The integrin $\alpha\beta 3$ expression level of U87MG cells was 99.98% (data not shown).

Cellular uptake of cRGD-siEGFR

Flow cytometry results (Figure 1C–E) showed that naked siRNA barely entered U87MG cells, with a Cy5-positive rate of 1.27% and a fluorescence intensity of 11.67, in accordance with the results of confocal microscopy. Compared with the naked siRNA-Cy5 group, U87MG cells had better ability to take up cRGD-siEGFR-Cy5 (100 nM), cRGD-siEGFR-Cy5 (400 nM) and Lipo2000/siRNA-Cy5 (100 nM), and the positive rate of uptake was 97.97%, 98.68% and 98.58%, respectively, and the fluorescence intensity was 347, 1145 and 3133, respectively. The uptake ability increased as the administration dose increased.

Gene knockdown efficiency of cRGD-siEGFR *in vitro*

Compared with the control group, EGFR mRNA in groups transfected with 500 nM, 800 nM, and 1000 nM cRGD-siEGFR decreased significantly (the expression level was 47.39%, 23.93%, 18.34%, respectively, $p < 0.01$, Figure 1F). In terms of the amount of conjugate used for transfections, the silencing efficacy of cRGD-siEGFR increased as the concentration rose; when the concentration reached 1000 nM, the silencing efficacy was higher than the Lipo2000/siRNA group, and the difference was significant ($p < 0.05$). Total protein was collected for western blot analysis after 72 h, and EGFR protein expression was significantly decreased in the cRGD-siEGFR group and Lipo2000/siRNA group, compared with control groups and the cRGD-siNC group (Figure 1G,H). Taken together, these results suggested that cRGD-siEGFR effectively inhibited EGFR expression in U87MG cells.

Inhibition of cell proliferation and promotion of apoptosis by cRGD-siEGFR *in vitro*

CCK-8 assay results showed that cRGD-siEGFR at different concentrations (600 nM and 800 nM) significantly inhibited the proliferation of U87MG cells at 48 h and 72 h ($p < 0.01$, Figure 2A). The inhibition of proliferation *in vitro* was also confirmed with an EDU experiment (Figure 2B,C).

Flow cytometry results showed that cRGD-siEGFR at different concentrations (400 nM, 600 nM and 800 nM) clearly induced apoptosis of U87MG cells *in vitro*, with apoptosis rates of 26.59%, 45.23% and 55.28%, respectively (Figure 2D,E). However, the results of the CCK-8 experiment showed that cRGD-siNC was of very low toxicity, as seen in supplementary Figure S2.

Bio-distribution and tumor vascular permeability of cRGD-siEGFR *in vivo*

The results of *in vivo* imaging of tumor-bearing mice showed that cRGD-siEGFR-Cy5 could specifically target tumors after intravenous injection (1 nmol/20 g). At 12 h and 24 h, a large amount of Cy5 fluorescence was observed at the tumor site; fluorescence was also observed in kidney tissue, as well as a

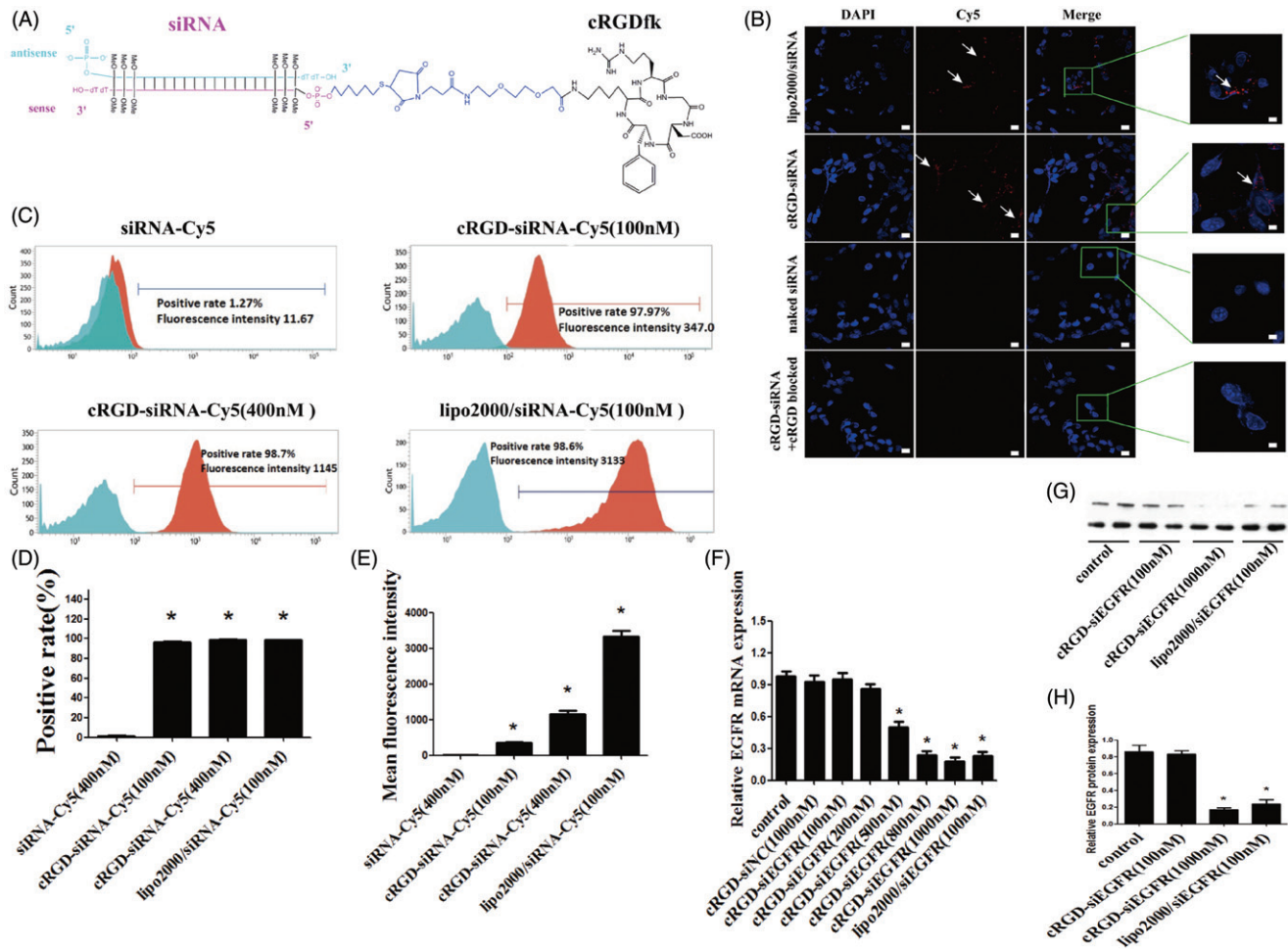


Figure 1. The schematic depiction, cell distribution, uptake and gene silencing efficiency of cRGD-siEGFR *in vitro*. (A) A diagram of cRGD-siEGFR conjugates. The cRGD moiety is conjugated to the 5'-phosphate of the passenger (sense) strand of EGFR siRNA through a thiol-maleimide linker. The backbone of EGFR-siRNA was modified with three 2'-O-Me on both ends of the sense strand and antisense strand. (B) Confocal laser scanning microscopy images of the intracellular distribution of cRGD-siEGFR. U87MG cells were transfected with Lipo2000/siRNA-Cy5, cRGD-siEGFR-Cy5, naked EGFR siRNA-Cy5, and for additional specificity tests, before being transfected with cRGD-siEGFR-Cy5, cells were pre-treated with 1 μ M unconjugated cRGD peptide (cRGD blocked). Cell nuclei were counterstained with DAPI (blue) and siRNA was labeled with Cy5 (red; marked by arrow). After 6 h of transfection, cells were fixed and visualized using confocal laser microscopy. (C) Cellular uptake levels of cRGD-siEGFR-Cy5 and siRNA-Cy5 in U87MG cells after 6 h of incubation with different ratios of cRGD-siEGFR-Cy5 and siRNA-Cy5, as measured by flow cytometry. Red area: fluorescence intensity related to cellular uptake of siRNA-Cy5. (D and E) Quantitative analysis of Cy5-positive expression levels and fluorescence intensity. * $p < 0.05$, compared with the siRNA-Cy5 group, $n = 3$. (F) Specific gene silencing *in vitro* for cRGD-siEGFR. U87MG cells were treated for 48 h with different concentrations of cRGD-siEGFR. (G and H) Quantitative analysis of EGFR protein expression levels. The expression of EGFR protein was calculated relative to the expression of GAPDH protein. * $p < 0.05$ vs. control group, # $p < 0.05$ vs. cRGD-siNC group, $n = 3$; bar = 20 μ m or 5 μ m.

small amount in liver tissue. However, 12 h to 72 h after injection with siRNA-Cy5, mice exhibited no Cy5 fluorescence at the tumor location. After dissection, consistent results were found, as shown in the images of organs and tissues *in vivo*. Both of the results indicated that cRGD-siEGFR could specifically target tumor tissue (Figure 3A).

After intravenous injection, cRGD-siEGFR-Cy5 could permeate into tumor stroma, while siRNA-Cy5 failed to enter tumor stroma (Figure 3B). In normal tissue, without expression of $\alpha v \beta 3$ receptors, and HeLa tumor tissue, cRGD-siEGFR failed to reach the tumor stroma. The integrin $\alpha v \beta 3$ expression level of HeLa cells was 4.29% (data not shown).

Anti-tumor activity of cRGD-siEGFR

The tumor-bearing mice were administered treatments 7 times *via* intravenous injection in the tail over a period of 48 h. The

tumor volume and body weight were measured before injection. On the third day after the last administration, the tumor volume and weight were measured again. The tumor growth curve is shown in Figure 4(A). There was no significant difference between the saline and cRGD-siNC treated groups, which demonstrated that cRGD-siNC did not have specific anti-tumor effects. Compared with saline-treated groups, cRGD-siEGFR (5 nmol/20 g) and cRGD-Vegfr2 siRNA (1.5 nmol/20 g) inhibited tumor growth significantly, beginning at 4 days after the second injection ($p < 0.05$), and low-dose cRGD-siEGFR (1.5 nM/20 g) inhibited tumor growth significantly beginning at 6 days after the third injection ($p < 0.05$).

The mice were euthanized three days after the last injection, and the tumors were excised and weighed (Figure 4B–D). The results showed that high-dose cRGD-siEGFR (5 nmol/20 g), cRGD-Vegfr2 siRNA (1.5 nmol/20 g)

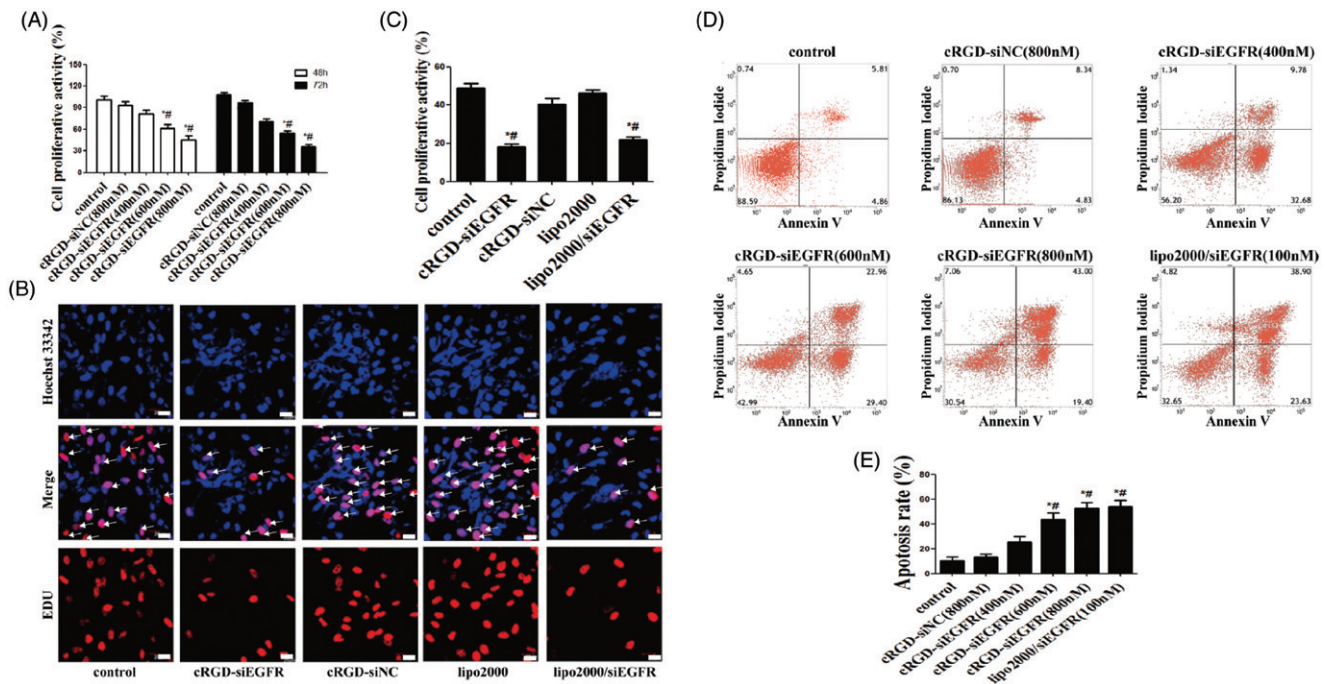


Figure 2. Cell proliferation and apoptosis *in vitro*. (A) Cell proliferation was detected with CCK-8. U87MG cells were incubated with different dosages of cRGD-siEGFR (400, 600 or 800 nM) and tested at 48 h or 72 h by a CCK-8 assay. Control was the untreated group. cRGD-siNC (800 nM) was the negative control group. (B) The proliferation of U87MG cells was detected by EDU after treatment with cRGD-siEGFR (800 nM) for 48 h. Control was the untreated group. cRGD-siNC (800 nM) was the negative control group. Treatment with siRNA (100 nM) using a transfection reagent (Lipo2000) was used as a knockdown positive control. A fluorescence image of cellular DNA (Hoechst stain; blue), and a fluorescence image of EdU-labeled DNA revealed by reaction with Alexa568 azide (red; marked by arrow). (C) Quantitative analysis of U87MG cell proliferation. The proliferative activity was relative to the fluorescence image of EdU-labeled DNA (red fluorescence; marked by arrow). (D) The apoptosis of U87MG cells was detected by flow cytometry after different treatments for 3 days. (E) Quantitative analysis of U87MG cell apoptosis. * $p < 0.05$ vs. Control group, # $p < 0.05$ vs. cRGD-siNC group, $n = 3$; bar = 20 μm .

and low-dose cRGD-siEGFR (1.5 nmol/20 g) significantly inhibited tumor growth, compared with the saline group; the weight or cumulative growth of the volume of tumors was reduced by approximately 50%, 32% and 27%, respectively. However, the nude mice treated with cRGD-Vegfr2 siRNA (1.5 nmol/20 g) combined with cRGD-siEGFR (1.5 nmol/20 g) had only slight inhibition of tumor growth ($p > 0.05$).

The results of qRT-PCR demonstrated an obviously low expression of EGFR mRNA in the cRGD-siEGFR (1.5 nmol/20 g) group and cRGD-siEGFR (5 nmol/20 g) group, when compared with the cRGD-siNC (5 nmol/20 g) or saline-treated group (Figure 5A). Furthermore, Figure 5(B,C) shows that the protein level was significantly decreased in the cRGD-siEGFR (1.5 nmol/20 g) group and cRGD-siEGFR (5 nmol/20 g) group. The results of a TUNEL assay demonstrated an obviously higher number of apoptotic cells in tumors from the mice treated with cRGD-siEGFR (5 nmol/20 g), cRGD-Vegfr2 siRNA (1.5 nmol/20 g) combined with cRGD-siEGFR (1.5 nmol/20 g) and cRGD-siEGFR (5 nmol/20 g), in comparison with mice treated with cRGD-siNC (5 nmol/20 g) or saline (Figure 4E). Immunohistochemical analysis using anti-EGFR antibody labeling also displayed a remarkably lower expression level of EGFR in tumors from mice treated with cRGD-siEGFR (5 nmol/20 g), cRGD-Vegfr2 siRNA combined with cRGD-siEGFR (1.5 nmol/20 g) and cRGD-siEGFR (5 nmol/20 g) compared with the mice treated with cRGD-siNC (5 nmol/20 g) or saline (Figure 5D). Taken together, the data show that cRGD-siEGFR can inhibit tumor growth effectively and specifically when administered

by intravenous injection in the tail. ELISA and blood biochemical test results showed that no significant difference in IFN- α , IFN- γ , IL-6, IL-12, Cr and ALT were found between the cRGD-siRNA group and control group (Figure S2B–D), suggesting low immunogenicity and toxicity of cRGD-siEGFR. Pathological section results further confirmed the low toxicity of cRGD-siRNA. Even though the mice were administered 7 times with a high dose (5 nmol/20 g), no serious toxicity to organs was found (Figure S2E).

Discussion

In this study, the purity of cRGD-siEGFR reached 78.7%–88.0%, but a purity of at least 90% is required if it is to be used as a drug. The low purity was associated with the small production scale (less than 100 nmol/lot). If the production amount was increased to more than 10 $\mu\text{mol/lot}$, synthetic purity may be significantly improved and be stable at more than 90% because the original impurities would not increase significantly with amplification of the production volume.

Unconjugated siRNA failed to penetrate the cell membrane and enter U87MG cells. However, cRGD-siRNA conjugates could enter cells through specific binding with $\alpha\text{v}\beta 3$ receptors. When $\alpha\text{v}\beta 3$ receptors were blocked, cRGD-siRNA failed to enter U87MG cells, suggesting that cRGD-siEGFR had high tumor-targeting ability compared with traditional tumor-targeting drugs. As part of a passive targeting system, nanoparticles and liposomes fail to target tumor cells

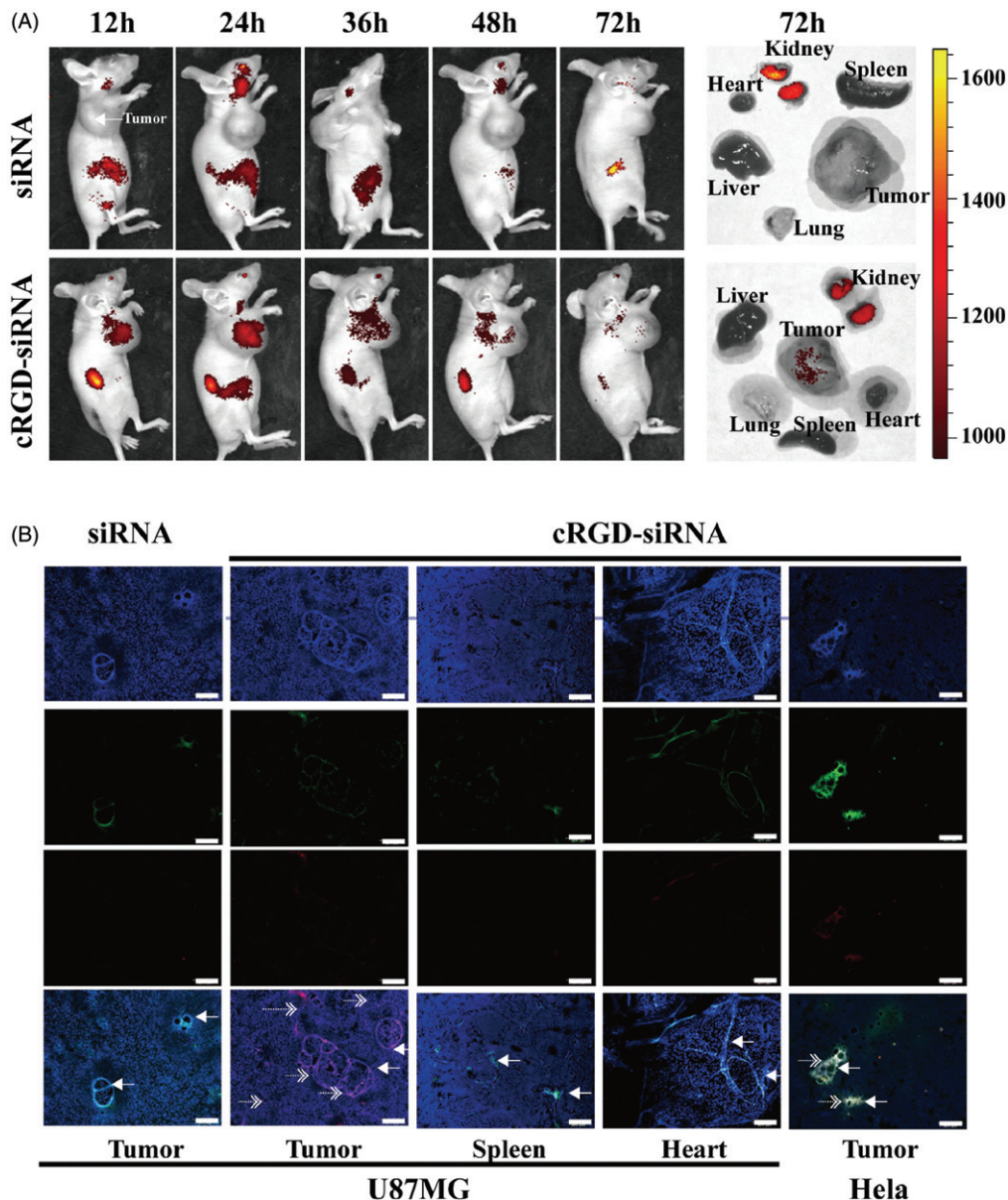


Figure 3. *In vivo* distribution and tumor vascular permeability of cRGD-siEGFR. (A) cRGD-siEGFR and un-conjugated siRNA bio-distributes to tumors. Nude mice bearing a U87MG tumor xenograft were injected with Cy5-labeled cRGD-siRNA conjugates or un-conjugated 2'-O-Me-stabilized siRNAs (tail vein, single dose, 1 nmol/20 g), and fluorescence images of whole animals or isolated organs were taken at indicated time points, 72 h after injection, using an IVIS imaging system. All images were scaled to the same minimum and maximum color values. (B) Tumor tissue targeting of cRGD-siRNA. Nude mice (female, 4–6 weeks, ~20 g) were inoculated subcutaneously on the right back with 5×10^6 U87MG or HeLa cells. When tumor volume reached 120 mm^3 , the animals were randomized into different groups for treatment testing. Mice bearing U87MG tumors were injected with either cRGD-siEGFR-Cy5 (1 nmol/20 g) or EGFR siRNA-Cy5 (1 nmol/20 g). Mice bearing HeLa tumors were injected with cRGD-siEGFR-Cy5 (1 nmol/20 g). Animals were euthanized 24 h after treatment. Tumor tissue was stained with DAPI (blue-fluorescence), blood vessels were marked with CD31 (green-fluorescence; marked by left arrow), and siRNA was labeled with Cy5 (red fluorescence; marked by right arrow); bar = 200 μm .

efficiently and specifically (Kanasty et al., 2013). In this regard, additional biological materials need to be added for the formation of stable nanoparticles and liposomes, which may result in adverse reactions and toxicity (Knudsen et al., 2015). However, compared with nanoparticles and liposomes, the cRGD-siEGFR conjugates were characterized by a definite molecular structure, molecular components and less toxicity. *In vitro* cytotoxicity was tested by exposing U87MG cells to increasing cRGD-siNC concentrations (50, 100, 200, 500, 1000, 1500 and 2000 nM), and this induced very low toxicity. The average viability of the cells was more than 90% at a concentration of 1000 nM (Figure S2A).

Our results showed that EGFR expression in U87MG cells was specifically silenced by cRGD-siEGFR with an IC_{50} of 500 nM. Moreover, the silencing efficacy reached 80% or above at the concentration of 1000 nM. In our previous study (Liu et al., 2014), an experiment was conducted in HUVEC lines with Vegfr2 mRNA as the target, and the IC_{50} of cRGD-siVegfr2 for Vegfr2 mRNA was lower than 100 nM. The inconsistency may be explained by the following reasons: (1) The target was different. Vegfr2 is an epidermal growth factor receptor for neovascularization, while EGFR is an epidermal growth factor receptor for cells; (2) Characteristics of HUVECs and U87MG cells are different. HUVECs are a

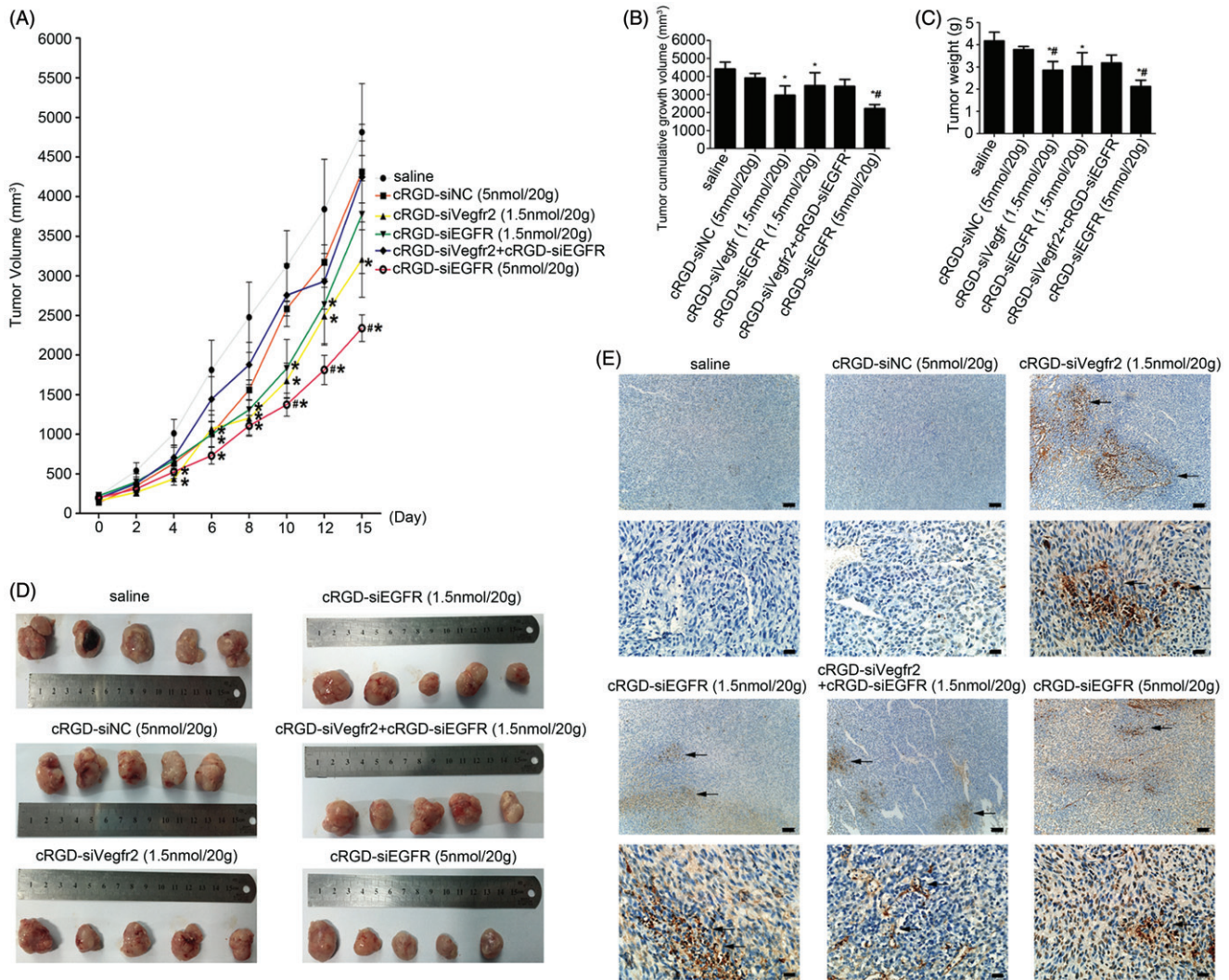


Figure 4. Anti-tumor activity of cRGD-siEGFR *in vivo*. (A) The tumor growth curve. Nude mice were repeatedly administered treatments (7 times) *via* intravenous injection in the tail, over an interval of 2 days. The tumor volume was measured before each injection. The growth curves were plotted as the mean tumor volume \pm SD (standard deviation). (B) The cumulative growth of tumor volume. The cumulative growth volume is equal to the volume of a tumor three days after the last injection minus the volume of the tumor before injection. (C) Tumor weight. The mice were euthanized three days after the last injection, and the tumor was excised, weighed and photographed (D). (E) Apoptosis in tumor tissue was detected by TUNEL staining. The apoptotic cells were brown under a light microscope; bar = 100 μ m or 20 μ m.

type of human umbilical vein endothelial cell and the U87MG cell line belongs to a malignant glioma cell line; (3) The difference in the siRNA sequence may affect the silencing efficiency. For instance, some of the sequences may possess a silencing rate of more than 95%, while others may only have approximately 30% (Angart et al., 2013); (4) The difference in the expression level of target mRNA. Further validation supported that, under the same procedures of RNA extraction and 40 cycles of amplification, the expression level of EGFR mRNA in U87MG cells was 3.2×10^5 times that with VEGFR2 mRNA in the HUVEC cell line (data not shown).

The metabolism research suggested that cRGD-siEGFR was effective at targeting tumors and had a high aggregation at tumor sites after 12 h, 24 h and 48 h. The primary organ for metabolism of the conjugates was the kidney, followed by the liver, and some metabolism was observed in other parts of the body. Confocal microscopy also found that cRGD-siEGFR only aggregated around tumor tissues that had high expression of $\alpha v \beta 3$ receptors, while no such aggregation was found in

normal tissues or tumor tissues with low $\alpha v \beta 3$ receptor expression. Compared with normal nanoparticles and liposomes, cRGD-siEGFR highly and specifically targeted tumors (Dahlman et al., 2014; Fehring et al., 2014).

In the current study, a U87MG cell tumor model was subcutaneously injected into nude mice. U87MG is a type of glioma cell line with its origin in the intracalvarium. Whether cRGD can penetrate into intracalvarial tumor tissues, through the blood brain barrier, was not investigated in our study. Zhang et al. demonstrated that cRGD was able to penetrate into intracalvarial tumor tissues, through the blood brain barrier into intracranial gliomas, and the expression of cRGD in tumor tissues was much higher compared with that in normal brain tissue (Zhang et al., 2011; Wang et al., 2015).

In the present study, we designed a cRGD-Vegfr2 siRNA combined with cRGD-siEGFR treatment group, which could theoretically have a synergistic anti-tumor effect. Our previous studies confirmed that cRGD-siVegfr2 can inhibit angiogenesis of tumors, thereby cutting off the oxygen and nutrient

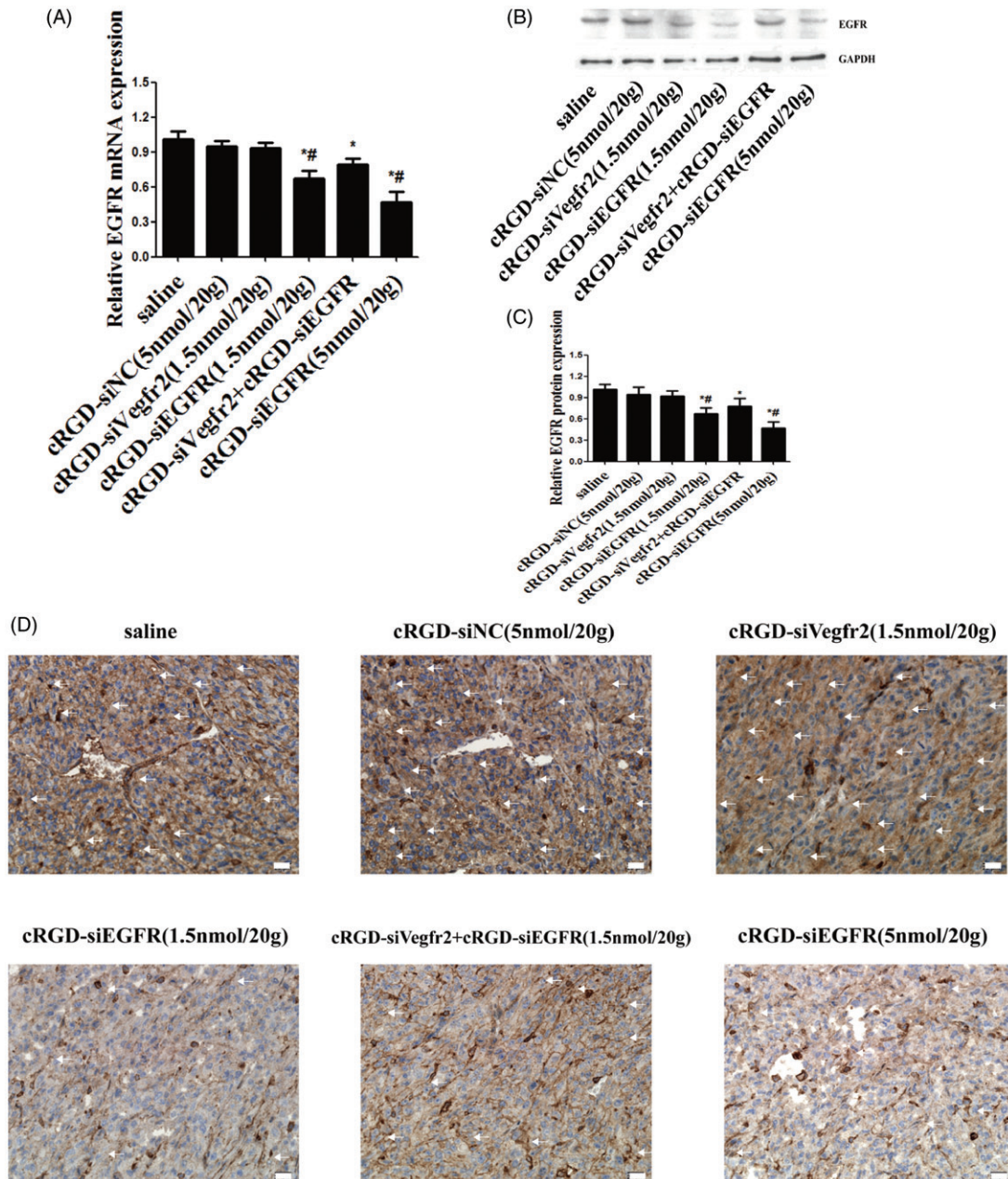


Figure 5. Gene silencing of cRGD-siEGFR *in vivo*. (A) qRT-PCR analysis of the EGFR mRNA levels expressed in tumors. EGFR mRNA expression was normalized to GAPDH mRNA. (B) Western blot analysis of EGFR protein expressed in tumors. (C) Quantitative analysis of EGFR protein expression levels. The expression of EGFR protein was calculated relative to the expression of GAPDH protein. (D) The relative expression level of EGFR protein in tumor tissue was detected by immunohistochemical staining. Anti-EGFR antibody (ab52894) is shown as brown (marked by arrow). * $p < 0.05$ vs. control group, # $p < 0.05$ vs. cRGD-siNC group, $n = 3$; bar = 20 μm .

supply for tumor tissue, leading to apoptosis of tumor cells and, ultimately, inhibition of tumor growth (Liu et al., 2014). cRGD-siEGFR directly inhibited tumor cell proliferation and induced tumor cell apoptosis, thereby inhibiting tumor growth. The combination of the two might directly and indirectly inhibit tumor growth. The results of this study, however, showed that there was no significant difference in tumor size in the combined drug group compared with the cRGD-siVegfr2 or cRGD-siEGFR alone groups. Even worse, there was no significant difference between the combined treatment group and the control or cRGD-siNC group. The possible reasons for this might include the following two reasons. (1) The dose of both drugs was insufficient. We gave a combined dose of 1.5 nmol/20 g, but the results of the

experiment showed that only a dose as high as 5 nmol/20 g significantly suppressed tumor growth. Therefore, a low dose of the two drugs combined could not induce a synergistic effect. Furthermore, because of competitive binding of cRGD-siEGFR and cRGD-siVegfr2 to the $\alpha v \beta 3$ receptor, the combination treatment group needs a much higher dose than that in the single drug groups to produce equivalent effects for inhibition of tumor growth. (2) Because cRGD-siVegfr2 inhibited the angiogenesis of tumors, cRGD-siEGFR could not effectively penetrate tumor tissue *via* vessels, which restricted the synergistic effect.

In this study, we examined the immune response of normal mice treated with 5 nmol/20 g of cRGD-siEGFR and tumor-bearing nude mice after administration (7 times) of

cRGD-siEGFR by measuring biochemical indicators of liver and renal toxicity. The blood biochemical test and ELISA results showed that no significant difference in Cr, ALT, IL-6, IL-12, IFN- α and IFN- γ were found between the experimental groups and the control group (Figure S2B–D), suggesting low toxicity of cRGD-siEGFR. Blood biochemical indicators only reflected real-time damage, but there was no evidence of already-present injury or damage in the recovery time; therefore, we observed the pathological sections of the organs in each group of nude mice, and no serious toxicity to organs was found, even in the high-dose (5 nmol/20 g) group (Figure S2E). However, some mild adverse effects were found. For example, pathological sections of kidney indicated that the glomerular filtration ability was disturbed in the high-dose (5 nmol/20 g) group. Previous studies have found that glomerular epithelial cells in healthy humans express $\alpha 1$, $\alpha 3$, $\alpha 5\beta 1$, $\alpha v\beta 3$ and $\alpha v\beta 5$ integrin receptors (Hamerski & Santoro, 1999). This suggests that cRGD-siEGFR can reach the kidney and be taken up by glomerular epithelial cells. In addition, peptides and low molecular weight proteins, such as cRGD peptides, are filtered by glomeruli. Following this, molecules can be reabsorbed into the renal cortex and the surrounding capillaries in proximal tubules (Briat et al., 2012). Hence, the accumulation of cRGD-siEGFR in the kidney and renal toxicity in the renal cortex may be caused by these factors. Tubular epithelial cells are among the non-immune cells that express TLR1, -2, -3, -4 and -6, suggesting that TLRs might contribute to the activation of immune responses in renal injury (Anders, 2004). Injury of glomerular filtration function with the high-dose (5 nmol/20 g) of conjugate probably occurred because the 21-nucleotide siRNA interacted with TLR3 in the glomerular endothelial cells, thus activating the innate immune response and causing kidney damage, resulting in renal toxicity (Kleinman et al., 2008).

Taken together, our results provide strong evidence for the potential use of cRGD-siRNA to target EGFR in glioma as an anticancer therapeutic. However, several studies will need to be conducted to take this therapeutic to the next stage of drug development. These studies might include (i) increasing the potency of siRNA and limiting the total dose delivered to patients to reduce immunogenicity and toxic effects; (ii) extending the dosing interval, which would increase the time available to repair sub-lethal damage; (iii) optimizing the siRNA backbone to reduce the association of the siRNA molecule with TLR3 in renal tubular endothelial cells and, thus, reduce the nephrotoxicity likely caused by the immunogenicity; and (iv) administering the conjugate with other drugs, such as Gelofusine, to reduce renal reabsorption of cRGD-siRNA, thereby reducing renal toxicity (Briat et al., 2012; Lee et al., 2015).

Conclusions

We have demonstrated that cRGD-siEGFR can effectively knockdown EGFR expression with high tumor uptake *in vitro* and *in vivo*. In addition, after systemic intravenous delivery of cRGD-siEGFR, we showed that down-regulation of EGFR in mouse tumors could substantially slow tumor growth, and low toxicity or innate immune response was induced *in vivo*.

Collectively, cRGD-siEGFR represents a novel tumor-targeting delivery system for siRNAs and a promising candidate for cancer therapy.

Declaration of interest

The authors have no conflict of interest.

This work was supported in part by National Nature Science Foundation of China [NSFC81370449] and Science and Technology Program of Guangdong Province [2013B091300014].

References

- Ahmed MS, Bae YS. (2014). Dendritic cell-based therapeutic cancer vaccines: past, present and future. *Clin Exp Vaccine Res* 3:113–16.
- Alam MR, Ming X, Fisher M, et al. (2011). Multivalent cyclic RGD conjugates for targeted delivery of small interfering RNA. *Bioconjug Chem* 22:1673–81.
- Anders HJ. (2004). Signaling danger: toll-like receptors and their potential roles in kidney disease. *J Am Soc Nephrol* 15:854–67.
- Angart P, Vocelle D, Chan C, Walton S. (2013). Design of siRNA therapeutics from the molecular scale. *Pharmaceuticals (Basel)* 6: 440–68.
- Briat A, Wenk CHF, Ahmadi M, et al. (2012). Reduction of renal uptake of ¹¹¹In-DOTA-labeled and A700-labeled RAFT-RGD during integrin $\alpha v\beta 3$ targeting using single photon emission computed tomography and optical imaging. *Cancer Sci* 103:1105–10.
- Cetin B, Gumusay O, Cengiz M, Ozet A. (2016). Advances of molecular targeted therapy in gastric cancer. *J Gastrointest Cancer* 47:125–34.
- Choi YJ, Lee DH, Choi CM, et al. (2015). Randomized phase II study of paclitaxel/carboplatin intercalated with gefitinib compared to paclitaxel/carboplatin alone for chemotherapy-naïve non-small cell lung cancer in a clinically selected population excluding patients with non-smoking adenocarcinoma or mutated EGFR. *Bmc Cancer* 15:763.
- Dahlman JE, Barnes C, Khan OF, et al. (2014). In vivo endothelial siRNA delivery using polymeric nanoparticles with low molecular weight. *Nat Nanotechnol* 9:648–55.
- Dechantsreiter MA, Planker E, Matha B, et al. (1999). N-Methylated cyclic RGD peptides as highly active and selective $\alpha(V)\beta(3)$ integrin antagonists. *J Med Chem* 42:3033–40.
- Fehring V, Schaeper U, Ahrens K, et al. (2014). Delivery of therapeutic siRNA to the lung endothelium via novel Lipoplex formulation DACC. *Mol Ther* 22:811–20.
- Guo C, Manjili MH, Subjeck JR, et al. (2013). Therapeutic cancer vaccines: past, present, and future. *Adv Cancer Res* 119:421–75.
- Hamerski DA, Santoro SA. (1999). Integrins and the kidney: biology and pathobiology. *Curr Opin Nephrol Hypertens* 8:9–14.
- Horiike A, Yamamoto N, Tanaka H, et al. (2014). Phase II study of erlotinib for acquired resistance to gefitinib in patients with advanced non-small cell lung cancer. *Anticancer Res* 34:1975–81.
- Hudis CA. (2007). Trastuzumab—mechanism of action and use in clinical practice. *N Engl J Med* 357:39–51.
- Jonker DJ, Karapetis CS, Harbison C, et al. (2014). Epiregulin gene expression as a biomarker of benefit from cetuximab in the treatment of advanced colorectal cancer. *Br J Cancer* 110:648–55.
- Kanasty R, Dorkin JR, Vegas A, Anderson D. (2013). Delivery materials for siRNA therapeutics. *Nat Mater* 12:967–77.
- Kleinman ME, Yamada K, Takeda A, et al. (2008). Sequence- and target-independent angiogenesis suppression by siRNA via TLR3. *Nature* 452:591–7.
- Knudsen KB, Northeved H, Kumar EK P, et al. (2015). In vivo toxicity of cationic micelles and liposomes. *Nanomedicine* 11:467–77.
- Le Tourneau C, Delord JP, Goncalves A, et al. (2015). Molecularly targeted therapy based on tumour molecular profiling versus conventional therapy for advanced cancer (SHIVA): a multicentre, open-label, proof-of-concept, randomised, controlled phase 2 trial. *Lancet Oncol* 16:1324–34.

- Lee SH, Kang YY, Jang H, et al. (2016). Current preclinical small interfering RNA (siRNA)-based conjugate systems for RNA therapeutics. *Adv Drug Deliv Rev* 104:78–92.
- Li J, Xue S, Mao Z-W. (2016). Nanoparticle delivery systems for siRNA-based therapeutics. *J Mater Chem B* 4:6620–39.
- Liang JL, Ren XC, Lin Q. (2014). Treating advanced non-small-cell lung cancer in Chinese patients: focus on icotinib. *Onco Targets Ther* 7: 761–70.
- Liu L, Liu X, Xu Q, et al. (2014). Self-assembled nanoparticles based on the c(RGDfk) peptide for the delivery of siRNA targeting the VEGFR2 gene for tumor therapy. *Int J Nanomedicine* 9: 3509–26.
- Liu X, Wang W, Samarsky D, et al. (2014). Tumor-targeted in vivo gene silencing via systemic delivery of cRGD-conjugated siRNA. *Nucleic Acids Res* 42:11805–17.
- Louis DN. (2006). Molecular pathology of malignant gliomas. *Annu Rev Pathol* 1:97–117.
- Maemondo M, Inoue A, Kobayashi K, et al. (2010). Gefitinib or chemotherapy for non-small-cell lung cancer with mutated EGFR. *N Engl J Med* 362:2380–8.
- Pietrantonio F, Perrone F, Biondani P, et al. (2013). Single agent panitumumab in KRAS wild-type metastatic colorectal cancer patients following cetuximab-based regimens: Clinical outcome and biomarkers of efficacy. *Cancer Biol Ther* 14: 1098–103.
- Salic A, Mitchison TJ. (2008). A chemical method for fast and sensitive detection of DNA synthesis in vivo. *Proc Natl Acad Sci USA* 105: 2415–20.
- Shen J, Kim H-C, Su H, et al. (2014). Cyclodextrin and polyethylenimine functionalized mesoporous silica nanoparticles for delivery of siRNA cancer therapeutics. *Theranostics* 4:487–97.
- Shen J, Xu R, Mai J, et al. (2013). High capacity nanoporous silicon carrier for systemic delivery of gene silencing therapeutics. *ACS Nano* 7:9867–80.
- Shimaoka M, Xiao T, Liu JH, et al. (2003). Structures of the alpha L I domain and its complex with ICAM-1 reveal a shape-shifting pathway for integrin regulation. *Cell* 112:99–111.
- Wang K, Zhang X, Zhang L, et al. (2015). Development of biodegradable polymeric implants of RGD-modified PEG-PAMAM-DOX conjugates for long-term intratumoral release. *Drug Deliv* 22:389–99.
- Wang Y, Xiao W, Zhang Y, et al. (2016). Optimization of RGD-containing cyclic peptides against alphavbeta3 integrin. *Mol Cancer Ther* 15:232–40.
- Xu N, Fang W, Mu L, et al. (2016). Overexpression of wildtype EGFR is tumorigenic and denotes a therapeutic target in non-small cell lung cancer. *Oncotarget* 7:3884–96.
- Zhang L, Zhu S, Qian L, et al. (2011). RGD-modified PEG-PAMAM-DOX conjugates: in vitro and in vivo studies for glioma. *Eur J Pharm Biopharm* 79:232–40.

Supplemental data available online